

# Optothermal Properties of Fibers. IV. Optical Properties of Nylon 66 Fibers as a Function of Quenching Process

I. M. FOU DA,<sup>1,\*</sup> M. M. EL-NICKLAWY,<sup>2</sup> E. M. NASR,<sup>2</sup> and R. M. EL-AGAMY<sup>2</sup>

<sup>1</sup>Physics Department, Faculty of Science, Mansoura University, Mansoura, Egypt, and <sup>2</sup>Physics Department, Faculty of Science, Helwan University, Cairo, Egypt

## SYNOPSIS

In this work, optical properties of samples of nylon 66 fibers were quenched in coarse-grained ice after annealing in the temperature range 80–180°C for 1–10 h. Two independent techniques were used to study optical parameters in these fibers. The first technique is the application of the diffraction technique to study the effect of quenching on the swelling factors of these fibers for some different liquids at room temperature of  $25 \pm 1^\circ\text{C}$ . The second method dealt with the application of multiple-beam Fizeau fringes in transmission to estimate the refractive indices and birefringence of the skin and core of these fibers. The obtained results were utilized to calculate the polarizability per unit volume, isotropic refractive indices, and the Cauchy's dispersion constants. The relationship between  $n_s^{\parallel,\perp}$ ,  $n_c^{\parallel,\perp}$ ,  $n_a^{\parallel,\perp}$ ,  $\Delta n_s$ ,  $\Delta n_c$ ,  $\Delta n_a$ ,  $n_{(iso)s}$ ,  $n_{(iso)c}$ , and  $n_{(iso)a}$  and different annealing times and temperatures is given for these fibers. Microinterferograms and curves are also given. © 1996 John Wiley & Sons, Inc.

## INTRODUCTION

The measurement of optical anisotropy in polymers is one of the simplest and most exploited methods of studying orientation in these polymers. These optical properties vary with their directions in the fibers, especially along and perpendicular to the fiber axis because of the orientation of the fiber chain. Mechanical and thermal properties were found to be influenced by the optical heterogeneity of a solid.<sup>1</sup>

Many techniques have been used to determine the refractive indices and birefringence of fibers. In this respect, both two-beam and multiple-beam microinterferometry have been utilized by many authors.<sup>2–9</sup> Recently, Barakat and Hamza<sup>10</sup> concentrated on the fundamentals of interferometry and used the interferometric methods for optical synthetic and natural fiber analysis and research.

More recently, the application of double-beam and multiple-beam Fizeau fringes interferometry has

stimulated interest in studying the effect of different types of thermal and mechanical properties of natural and man-made fibers.<sup>11–15</sup> The most available technique for changing the polymeric structure is the annealing and quenching process.<sup>16–20</sup> The effects of annealing increases drastically with temperature, but also depends on the time the sample is held at the annealing temperature. Therefore, thermal treatment was used to vary the degree of crystallinity in polymeric materials.

Increases in order are produced by heating. Disorder is produced either by melting and quenching or by cold working. The disordered state of crystallizable polymer is often produced simply by quenching and some refer to it simply as quenched or shock-cooled material.<sup>21</sup>

In this work, the mechanism of optical changes in the orientation structure of nylon 66 fibers due to annealing and quenching in coarse ice pieces was determined interferometrically. Multiple-beam Fizeau fringes were used for the determination of the mean refractive indices ( $n_a^{\parallel}$  and  $n_a^{\perp}$ ), the skin refractive indices ( $n_s^{\parallel}$  and  $n_s^{\perp}$ ), and the core refractive indices ( $n_c^{\parallel}$  and  $n_c^{\perp}$ ) and for the birefringence in each

\* To whom correspondence should be addressed.

case for samples of nylon 66 fibers with different annealing conditions and quenching in coarse ice. The swelling absorption factor was also determined from its diffraction pattern using a He—Ne laser beam.

## THEORETICAL CONSIDERATIONS

### Interferometric Measurement of the Optical Parameters

Multiple-beam Fizeau fringes in transmission were used for the determination of the optical parameters for quenched nylon 66 fibers.

### Determination of Refractive Indices and Birefringence for the Nylon 66 Fiber Layers

*Nylon 66 Fibers with Circular Cross Section and Having Skin-Core Layers.* In this study, we measured the refractive indices and double refraction of annealed and quenched nylon 66 fibers by applying the following previously derived equation<sup>22</sup>:

$$\frac{dZ}{\Delta Z} = \frac{4}{\lambda} \sum_{k=0}^m A_k \quad (1)$$

where  $dZ$  is the value of the fringe shift;  $\Delta Z$ , the value of the order separation between two consecutive straight line fringes at the same point from the center of the fiber, and  $\lambda$ , the wavelength of the monochromatic light used:

$$A_k = (n_k - n_{k+1}) (r_k^2 - x^2)^{1/2}$$

where  $n_k$  = the refractive index of the layer  $k$  of the fiber,  $n_{k+1}$  = the refractive index of the medium in which the fiber is immersed (immersion of the liquid

**Table II** Refractive Indices  $n_s^{\parallel}$  and  $n_s^{\perp}$  and Birefringence  $\Delta n_s$  of the Skin of Untreated and Quenched Nylon 66 Fibers

State	$n_s^{\parallel}$	$n_s^{\perp}$	$\Delta n_s$
Untreated	1.5752	1.5237	0.0514
120°C 1 h	1.5792	1.5271	0.0522
120°C 2 h	1.5822	1.5269	0.0523
120°C 4 h	1.5799	1.5258	0.0541
120°C 6 h	1.5826	1.5273	0.0553
120°C 8 h	1.5814	1.5275	0.0539
120°C 10 h	1.5823	1.5255	0.0568

The wavelength of the light used was 546.1 nm at room temperature of  $25 \pm 1^\circ\text{C}$ . The error in measuring the liquid refractive index using an Abbe refractometer was  $\pm 0.0005$ .

$n_L$ ),  $r_k$  = the radius of the skin of order  $k$  from the core, and  $x$  = the distance measured from the center of the fringe shift and at which the shift tends to zero. Hence,

$$n_L = n_{k+1}, \quad n_0 = n_c, \quad r_m, \quad \text{and} \quad r_0 = r_c$$

where  $n_0$  is the refractive index of the central layer of the fiber (the core);  $r_f$ , the radius of the fiber; and  $r_m$  and  $r_f$ , the radius of the layers  $m$  and the central layer (core).

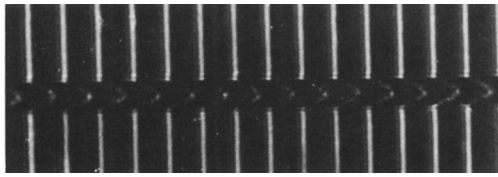
*The Mean Refractive Index  $n_a$ .* The mean refractive index  $n_a$  of the nylon 66 fibers, having a core of thickness  $t_c$  and refractive index  $n_c$ , surrounded by a skin layer of thickness  $t_s$  and refractive index  $n_s$ , is calculated using the following formula<sup>3</sup>:

$$n_a = n_c \frac{t_c}{t_f} + n_s \frac{t_s}{t_f} \quad (2)$$

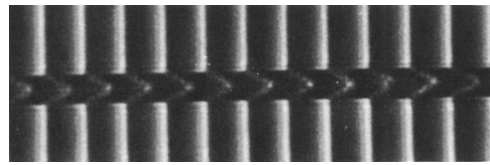
where  $t_f$  is the whole fiber thickness.

**Table I** Values of Swelling Factor for Untreated and Quenched Nylon 66 Fibers in Different Solvents

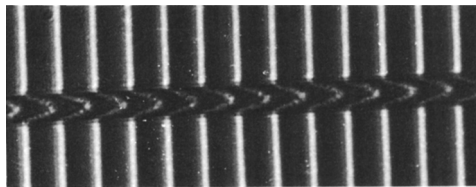
State	Sodium Carbonate Solution 20 g in 1 L Water	Water	Paraffin Oil	Acetic Acid 90% Concentration	Glycerin
Untreated	10	6.3	14.2	15.3	3.7
120°C 1 h	8.42	5.3	17.4	15.3	3.8
120°C 2 h	5.3	5.3	14.2	15.3	3.8
120°C 4 h	9.5	6.3	14.2	15.3	6.6
120°C 6 h	6.3	6.3	17.4	6.3	6.6
120°C 8 h	6.3	6.3	14.2	6.3	0.42
120°C 10 h	6.3	5.3	14.2	6.3	0.42



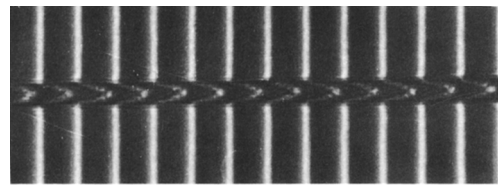
(a)



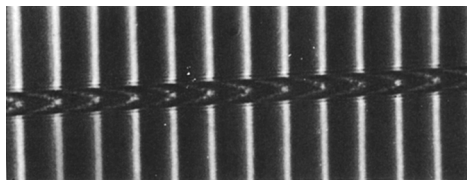
(b)



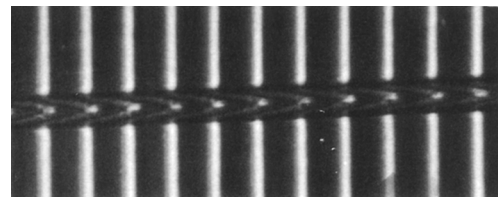
(c)



(d)



(e)



(f)

**Plate 1** (a-f) Microinterferograms of multiple-beam Fizeau fringes in transmission for quenched nylon 66 fibers with constant annealing temperature (80–180°C), using monochromatic light of wavelength 546.1 nm vibrating parallel and perpendicular to the fiber axis.

#### **Measurement of Swelling Factor of Quenching Nylon 66 Fibers by Laser-beam Diffraction**

In this method, the following formula<sup>23</sup> is used to determine the diameter:

$$d = \pm \lambda L/x \quad (3)$$

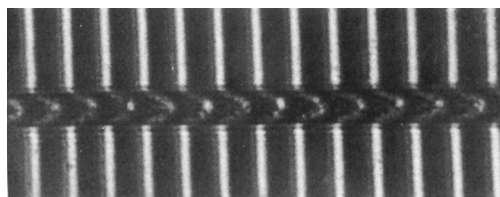
where  $d$  = is the fiber diameter,  $\lambda$  = the wavelength used,  $x$  = the distance from the center of the pattern to the first minimum, and  $L$  = the distance between

the fiber and the screen on which the pattern is produced.

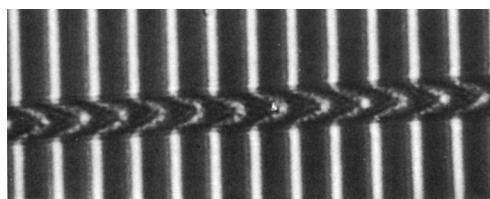
The following equation was used to determine the swelling factor<sup>24</sup>:

$$q = 100 (d_s - d_a)/d_a \quad (4)$$

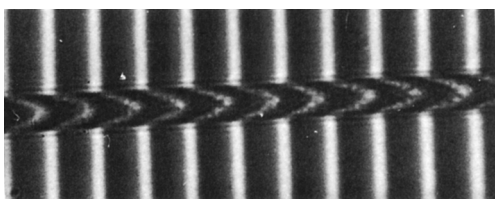
where  $d_s$  = diameter of swollen fiber and  $d_a$  = diameter of dry fiber. The results are tabulated in Table I.



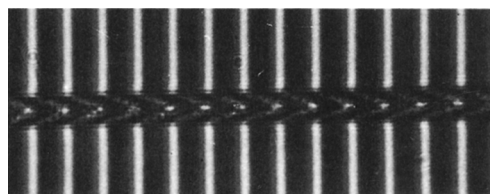
(a)



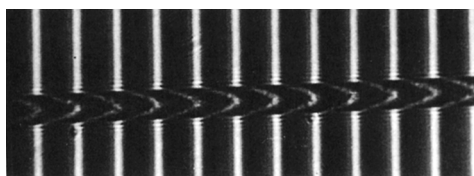
(b)



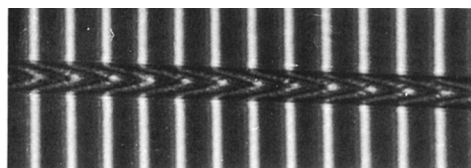
(c)



(d)



(e)



(f)

**Plate 2** (a-f) Microinterferograms of multiple-beam Fizeau fringes in transmission for quenched nylon 66 fibers with constant annealing temperature (80–180°C), using monochromatic light of wavelength 546.1 nm vibrating parallel and perpendicular to the fiber axis.

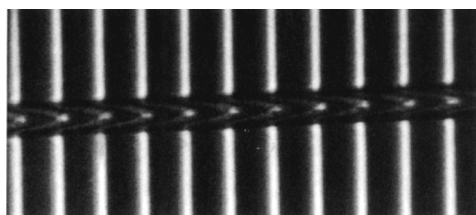
## EXPERIMENTAL AND RESULTS AND DISCUSSION

### Annealing and Quenching of Samples

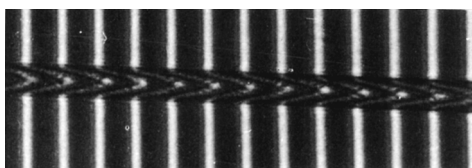
Samples of nylon 66 (I.C.I. polyamide 66 carded and combed) fibers were distributed in aluminum foil, which was then heated in an electric oven whose temperature was adjusted to be constant within  $\pm 1^\circ\text{C}$ . The samples were annealed at temperatures

ranging from 80 to 180°C for different annealing times ranging from 1 to 10 h. Every sample was then quenched in coarse ice pieces at a constant temperature (0°C).

A remarkable observation after 6 h was made when annealing nylon 66 fibers at a constant temperature (180°C): it became brittle; therefore, it was difficult to study it interferometrically after this occurrence.



(a)



(b)

**Plate 3** (a,b) Microinterferograms of multiple-beam Fizeau fringes in transmission for quenched nylon 66 fibers for a period of 10 h and at 120°C, using monochromatic light of wavelength 546.1 nm vibrating (a) parallel and (b) perpendicular to the fiber axis.

**The Refractive Indices  $n_s^{\parallel}$  and  $n_s^{\perp}$  and Birefringence  $\Delta n_s$  of the Outer Layer of Nylon 66 Fibers Measured by the Becke-line Method**

Using a monochromatic light of wavelength 546.1 nm, the immersion liquidly was prepared by mixing different volumes of  $\alpha$ -bromonaphthalene of refractive index  $n_1 = 1.6585$  at 20°C and liquid paraffin of refractive index  $n_2 = 1.4500$  at 20°C. For a mixture of the two liquids, 1 and 2, the refractive index of the mixture is  $n = (n_1 v_1 + n_2 v_2)/(v_1 + v_2)$ , where  $v_1$  and  $v_2$  are the volumes of liquids 1 and 2, respectively. The results are given in Table II. In the same table, the birefringence  $\Delta n_s$  is calculated for a set of quenched nylon 66 fibers having different annealing times at a constant temperature of 120°C. It is well known that the Becke-line method cannot determine the refractive indices for two directions on the same fiber. Two determinations are necessary: one parallel and the other perpendicular to the fiber axis. The optical effects produced by an immersed fiber do not depend solely upon the difference between the refractive indices of the fiber and the liquid, but also upon the product of this difference and the fiber thickness. Also, the Becke refractive indices are not confined to the fiber surface but may occur at any point on the fiber radius.<sup>25</sup>

**Multiple-beam Fizeau Fringes**

The method discussed in Ref. 10 for producing multiple-beam Fizeau fringes, formed by a silvered liquid

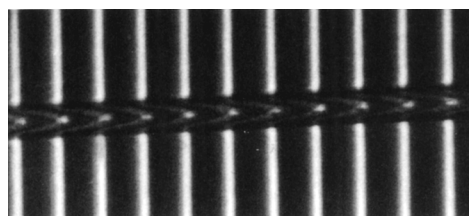
wedge crossing a fiber for the polarization plane of the light in parallel and perpendicular directions to the fiber axis, was used to measure the birefringence of annealed and quenched nylon 66 fibers.

Plate 1(a-f) show microinterferograms of multiple-beam Fizeau fringes in transmission for quenched nylon 66 fibers with a constant annealing time of 1 h and different annealing temperatures. A monochromatic light of wavelength 546.1 nm vibrating parallel to the fiber axis was used. In Plate 1(a-f), the immersion liquid was selected to allow the fringe shift to be small (within one to two orders of interference) and to determine accurately the point of connection of the fringe in the liquid and fiber regions. Plate 1(a-f) also shows that the fringe shift increases as the temperature of annealing increases.

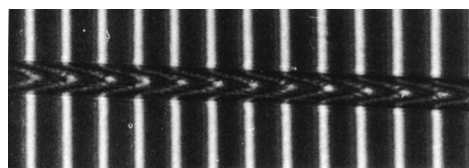
Plate 2(a-f) shows microinterferograms of multiple-beam Fizeau fringes in transmission for quenched nylon 66 fibers with a constant annealing time of 1 h and different annealing temperatures. A monochromatic light of wavelength 546.1 nm vibrating perpendicular to the fiber axis was used.

Plate 3(a,b) shows microinterferograms of multiple-beam Fizeau fringes in transmission for quenched nylon 66 fiber obtained by annealing for a period of time of 10 h at 120°C using a light vibrating parallel and perpendicular to the fiber axis.

Plate 4(a,b) shows microinterferograms of multiple-beam Fizeau fringes in transmission for quenched ny-



(a)



(b)

**Plate 4** (a,b) Microinterferograms of multiple-beam Fizeau fringes in transmission for quenched nylon 66 fibers for a period of 6 h and at 180°C, using monochromatic light of wavelength 546.1 nm vibrating (a) parallel and (b) perpendicular to the fiber axis.

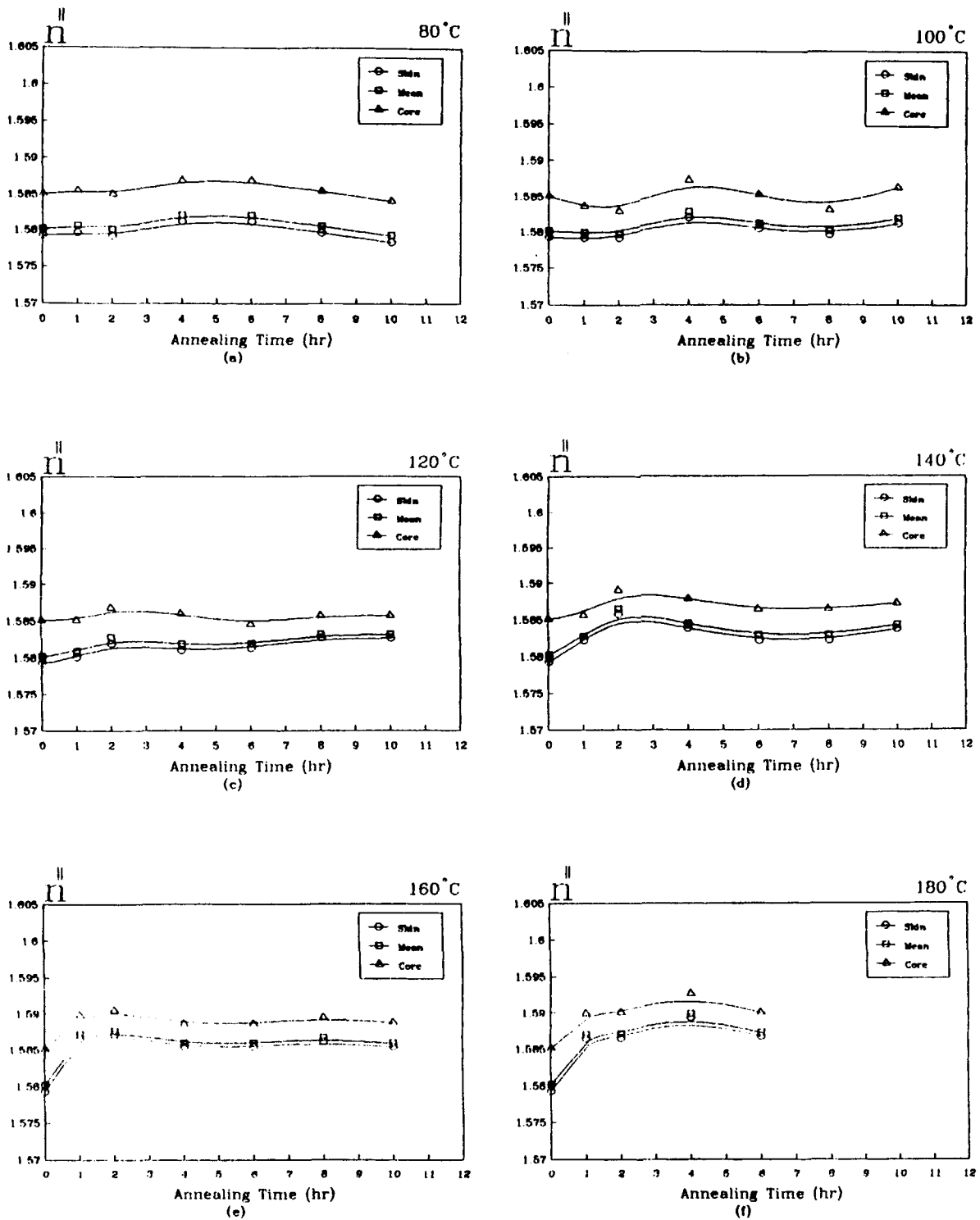
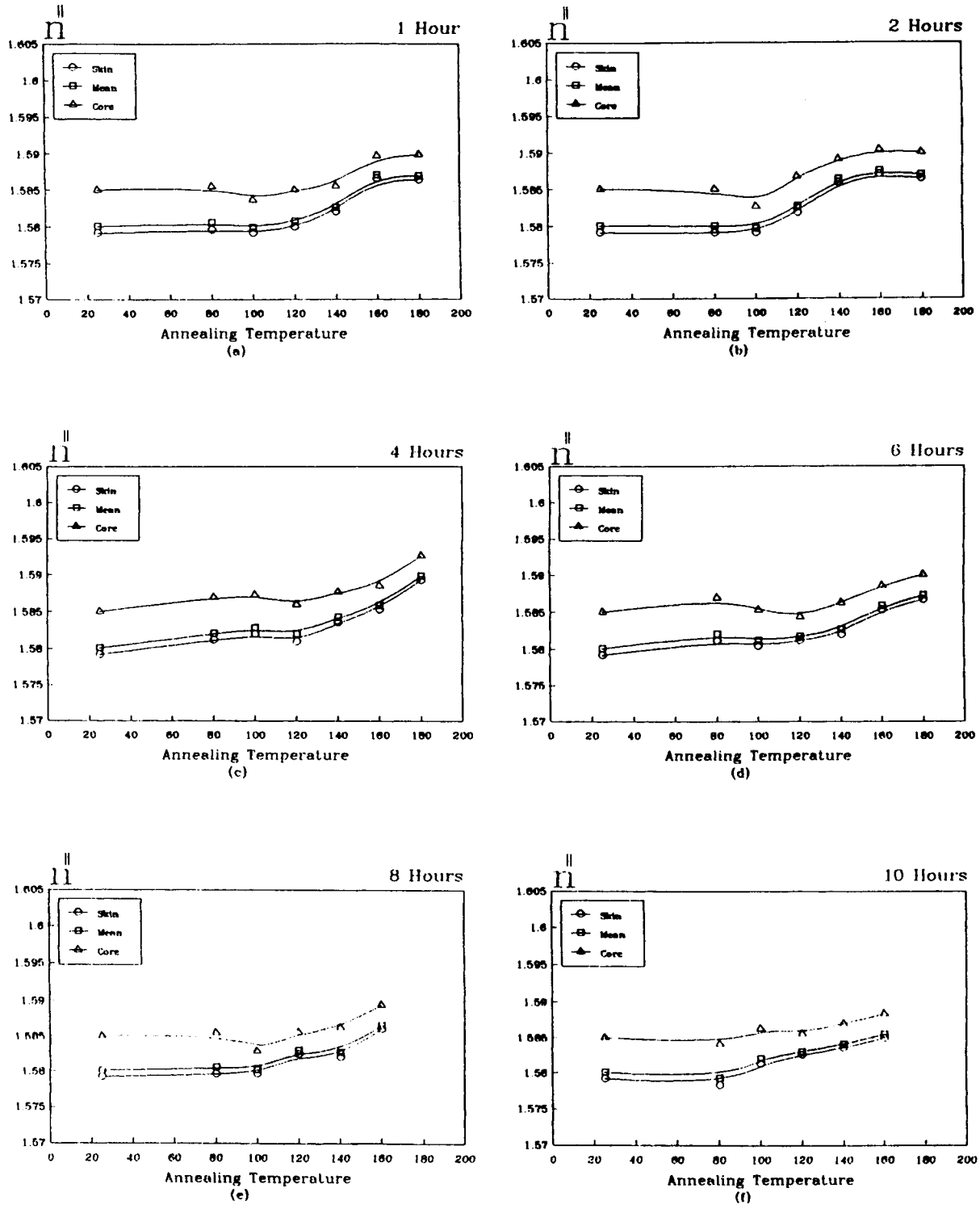
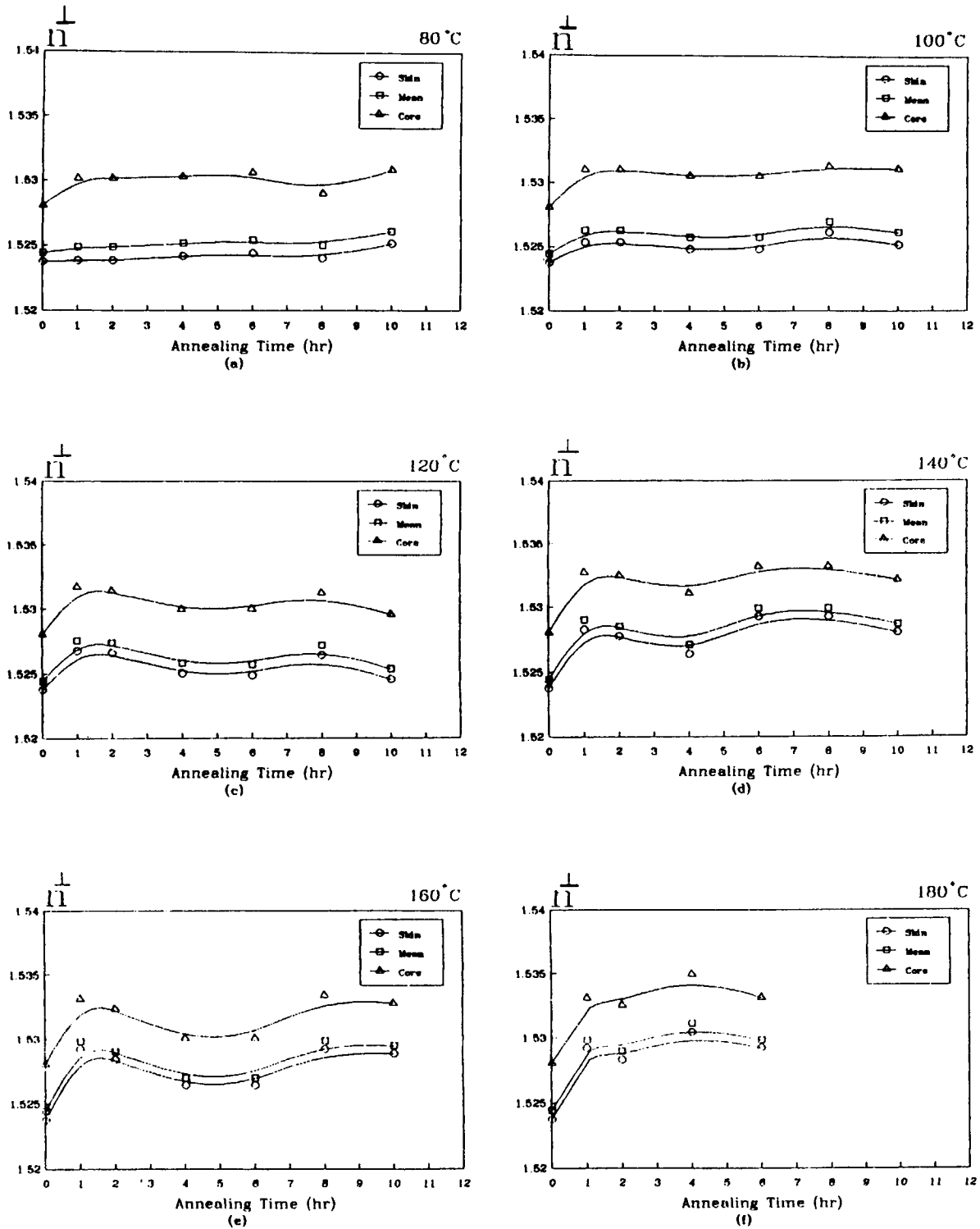


Figure 1 (a-f) Relation between annealing time (1-10 h) for different annealing temperatures (80-180°C) and quenching in coarse ice pieces (0°C) with refractive indices for light vibrating parallel to the fiber axis,  $n_{\parallel}^{\parallel}$ ,  $n_{\perp}^{\perp}$ , and  $n_{\text{av}}^{\text{av}}$ , of nylon 66 fibers.



**Figure 2** (a-f) Relation between annealing temperature (80-180°C) for different annealing times (1-10 h) and quenching in coarse ice pieces (0°C) with refractive indices for light vibrating parallel to the fiber axis,  $n_s^{\parallel}$ ,  $n_m^{\parallel}$ , and  $n_c^{\parallel}$ , of nylon 66 fibers.



**Figure 3** (a-f) Analogous forms to Figure 1(a-f), but for the light vibrating perpendicular to the fiber axis.



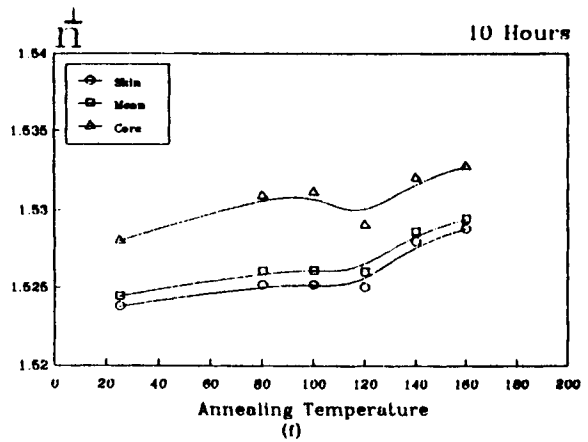
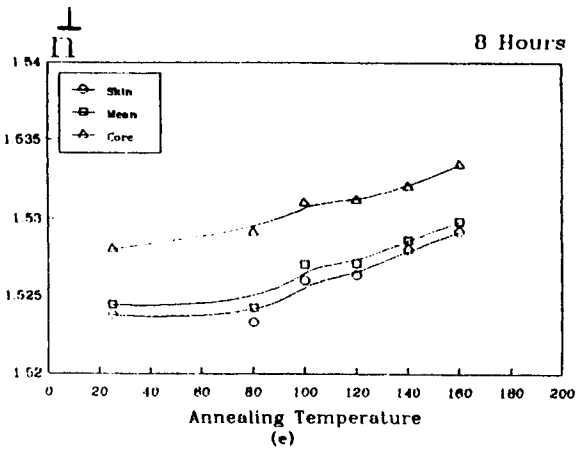
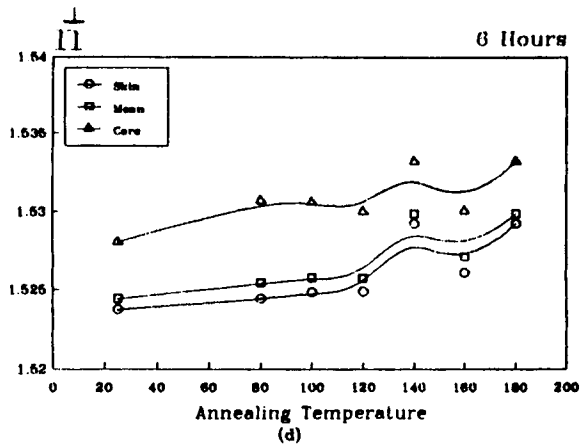
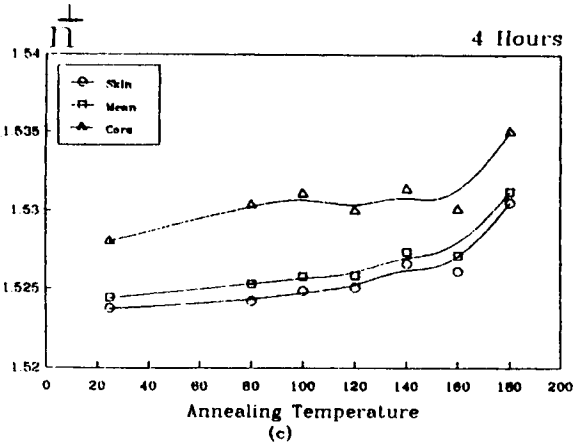
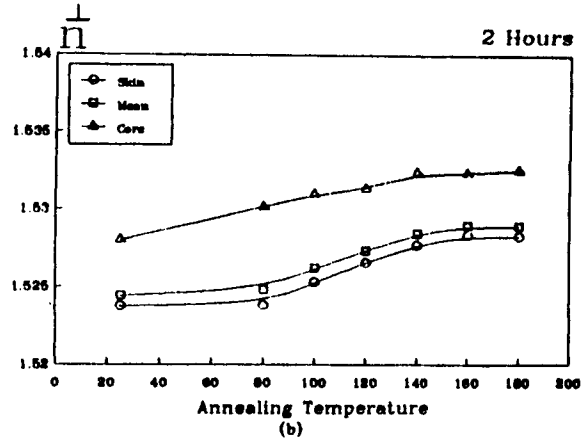
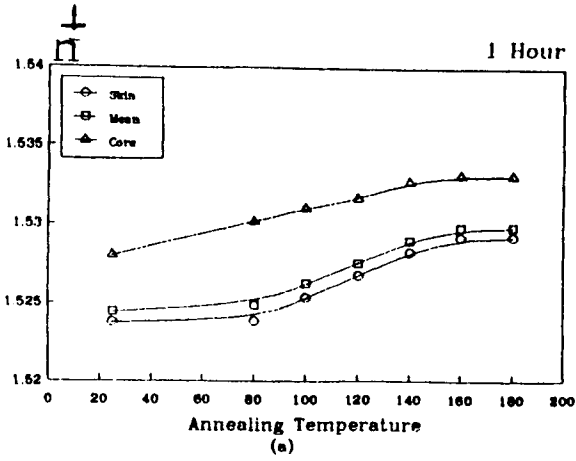


Figure 4 (a-f) Analogous forms to Figure 2 (a-f), but for the light vibrating perpendicular to the fiber axis.

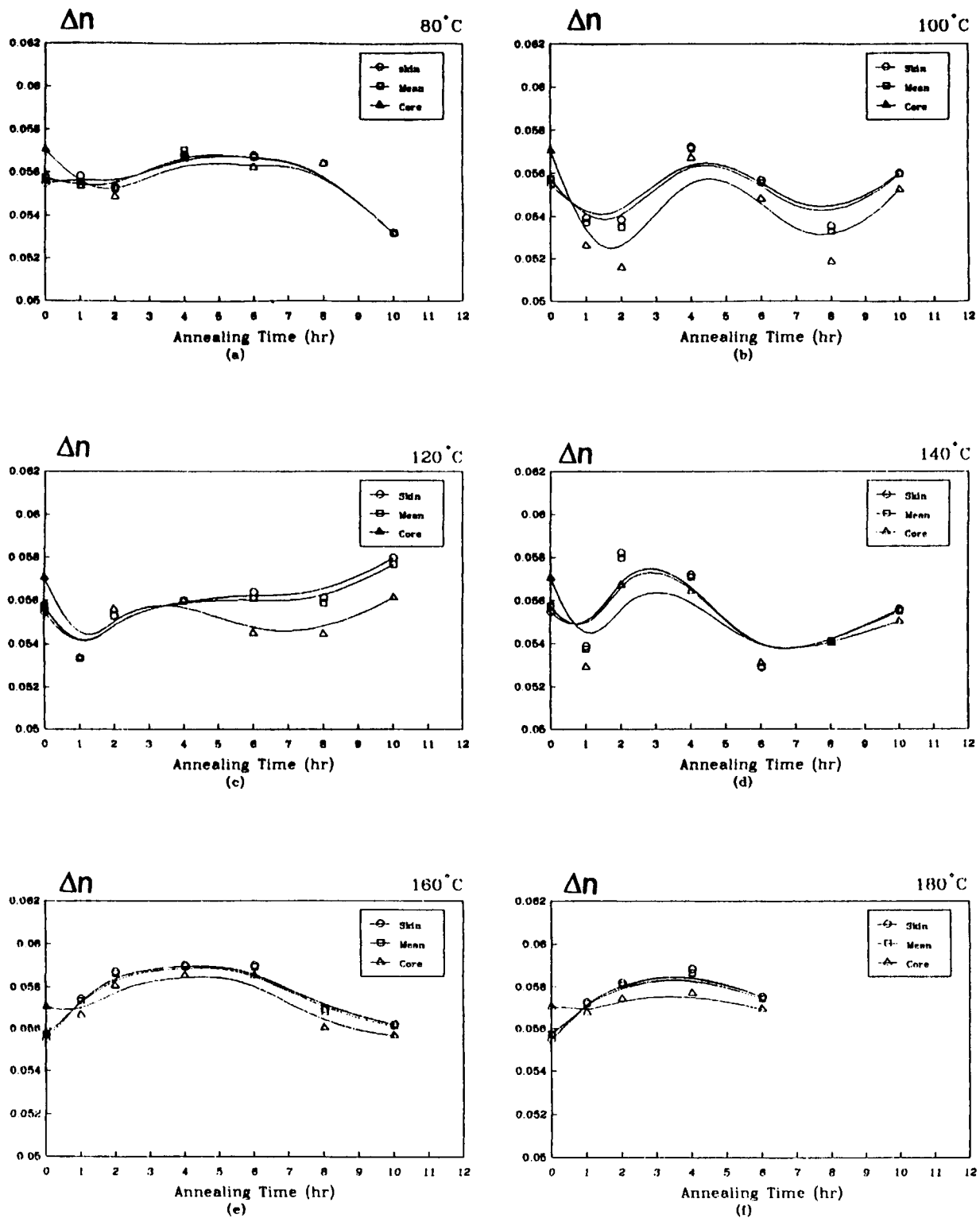


Figure 5 (a-f) Relation between quenched nylon 66 fibers and their birefringence at different times and constant temperatures.

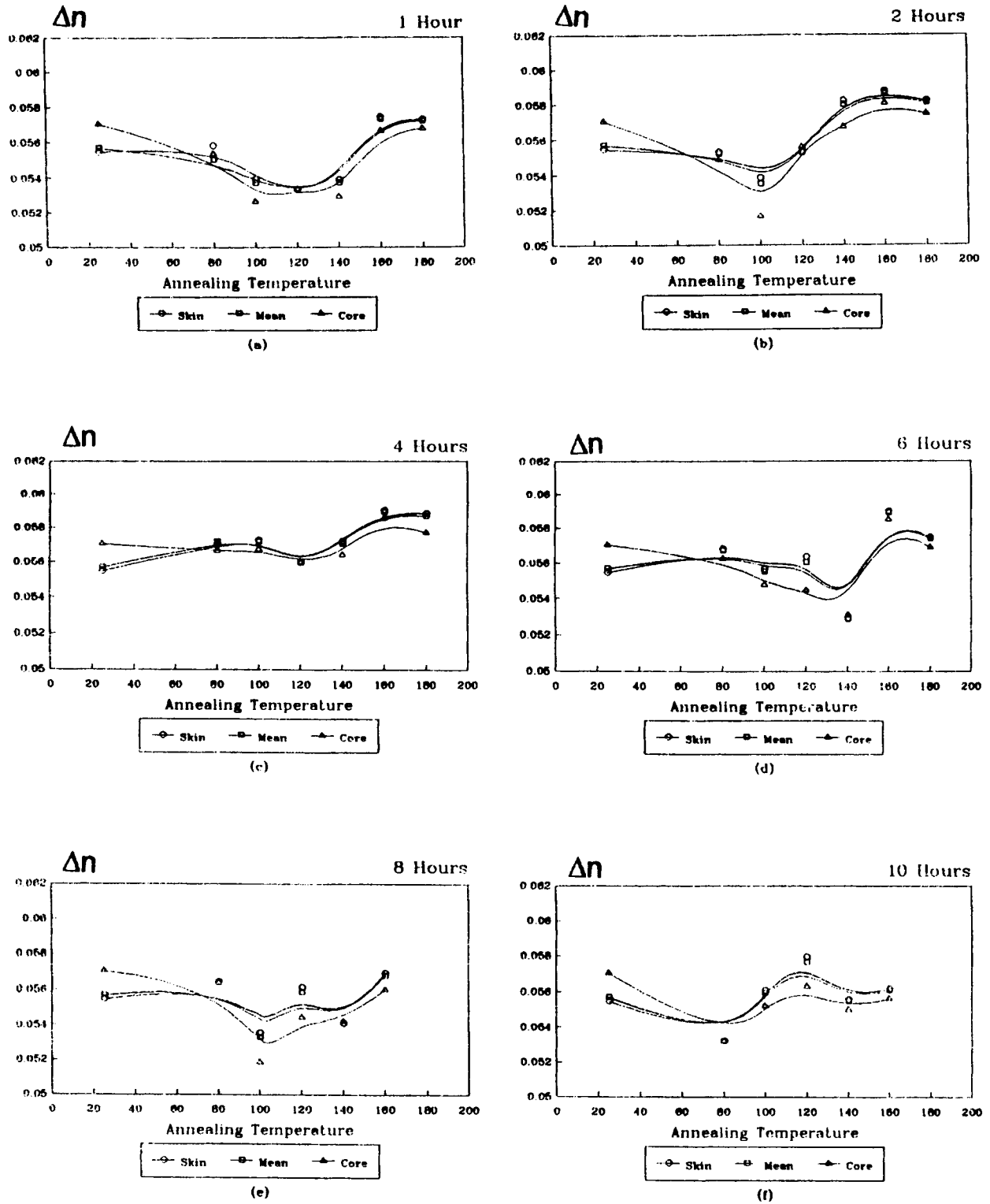
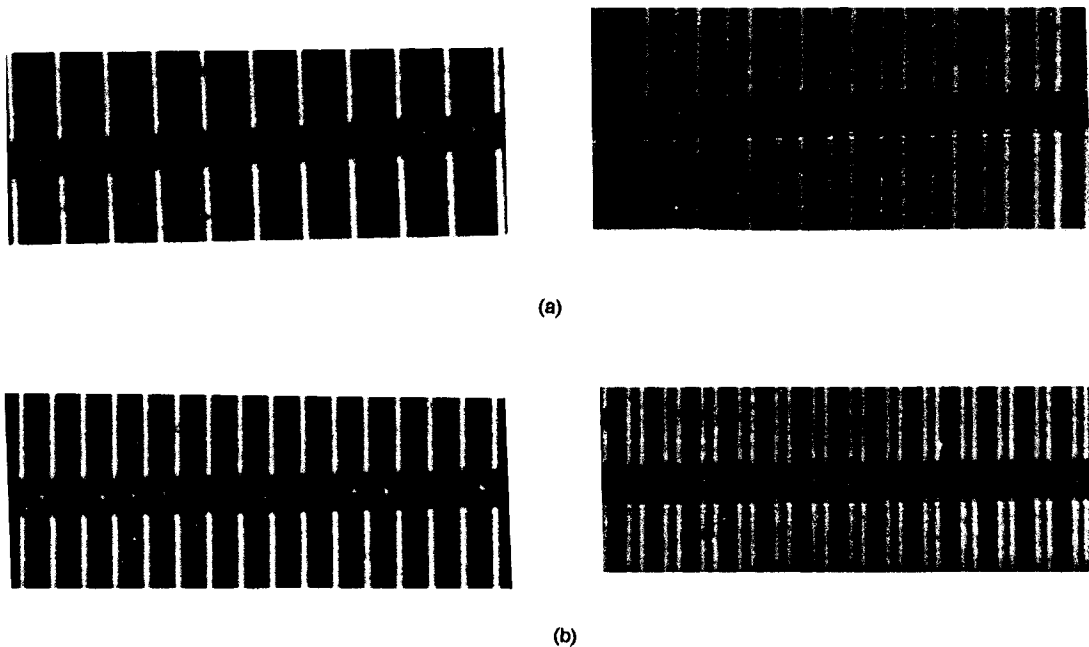


Figure 6 (a-f) Relation between quenched nylon 66 fibers and their birefringence at different temperatures and constant times.



**Plate 5** (a,b) Microinterferograms of multiple-beam Fizeau fringes in transmission for untreated nylon 66 fiber using monochromatic light of wavelengths 546.1, 577, and 579 nm vibrating (a) parallel and (b) perpendicular to the fiber axis.

lon 66 fiber obtained by annealing for a period of time of 6 h at 180°C using a light vibrating (a) parallel and (b) perpendicular to the fiber axis.

According to eq. (1), the fiber skin  $n_s^{\parallel,\perp}$  and core  $n_c^{\parallel,\perp}$  can be determined. Also, by applying eq. (2), the mean refractive indices  $n_a^{\parallel,\perp}$  can also be determined.

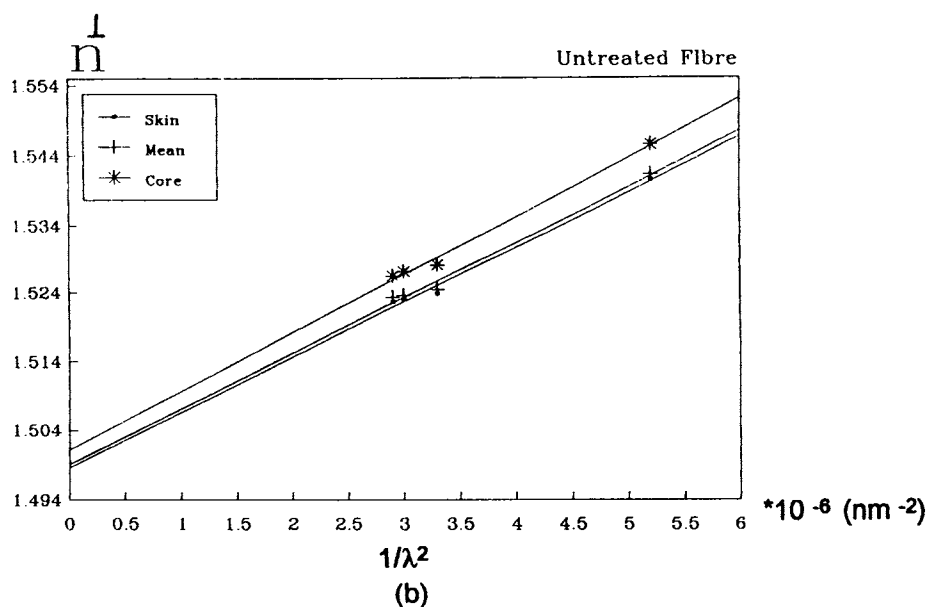
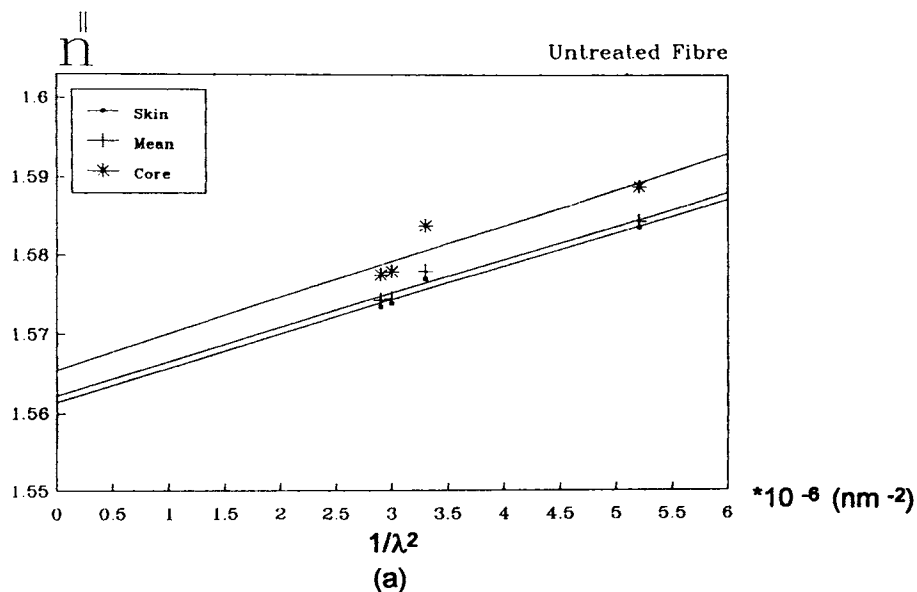
Figure 1(a–f) shows the variations of  $n_s^{\parallel}$ ,  $n_c^{\parallel}$ , and  $n_a^{\parallel}$  of nylon 66 fibers by increasing the annealing time (1–10 h) and annealing temperature (80–180°C) and quenching in coarse ice pieces, as obtained using multiple-beam Fizeau fringes in transmission. It is clear that annealing and quenching for 1 h at different ranges (80–180°C) leads to a slight increase in  $n_s^{\parallel}$ ,  $n_c^{\parallel}$ , and  $n_a^{\parallel}$  in most cases. The major mass redistribution could be observed in the period from 2–4 h. The curves in Figure 1(f) stopped after 6 h, as mentioned before.

Figure 2(a–f) shows the variations of  $n_s^{\parallel}$ ,  $n_c^{\parallel}$ , and  $n_a^{\parallel}$  of nylon 66 fibers by increasing the annealing temperature (80–180°C) and annealing time (1–10 h) and quenching in coarse ice pieces, as obtained using multiple-beam Fizeau fringes in transmission. Clearly observed is a transformation change when annealing samples of nylon 66 fibers at 100–120°C for different annealing periods and then quenching, which may be attributed to a change in the crystal

structure that can occur above  $T_g$  as  $T_m$  is approached. The drop or increase at 100–120°C could be explained as also due to a redistribution increase or decrease of the crystalline ratio to the amorphous ratio.

Figure 3(a–f) shows the variations of  $n_s^{\perp}$ ,  $n_c^{\perp}$ , and  $n_a^{\perp}$  of nylon 66 fibers obtained by the same technique as in Figure 1. But it is clear for the perpendicular direction that annealing and then quenching for 1 h from 80 to 180°C leads to increase of  $n_s^{\perp}$ ,  $n_c^{\perp}$ , and  $n_a^{\perp}$  and a decrease in the peak at 8, 6, 5, 4, 4.5, and 2 h for (a)–(f), respectively, with increasing annealing periods at the temperature ranges from 80 to 180°C. This behavior could be explained as due to the molecule's mobility to exhibit new rheological behaviors far from the unannealed and quenched material.

Figure 4(a–f) shows the variations of  $n_s^{\perp}$ ,  $n_c^{\perp}$ , and  $n_a^{\perp}$  of nylon 66 fibers obtained by the same technique as in Figure 2. It is clear that there are transitional temperature changes, due to the disordered state, which must be of concern for each case. Following the variability of every state, we could observe differences in temperature as shown: (a) and (b) 80°C, (c) 140°C, (d) 120°C, (e) 80°C, and (f) 100°C. This could be explained as due to the discontinuity of the heat flow through the skin of the fiber rather than



**Figure 7** (a,b) Variation of (a)  $n_s^{\parallel}$ ,  $n_c^{\parallel}$ , and  $n_a^{\parallel}$  and (b)  $n_s^{\perp}$ ,  $n_c^{\perp}$ , and  $n_a^{\perp}$  with  $1/\lambda^2$  for untreated nylon 66 fiber.

that through its core due to their difference in orientation and size distribution.

Figure 5(a-f) shows the relations between the annealed and quenched nylon 66 fibers and their birefringence at different times and constant temperature. A disorder state of orientation was produced by being shock-cooled (quenching) for different annealing temperatures and times. These dis-

ordered states may be due to the difference of the heat flow rate from the core to the skin and then to the surrounding medium from the skin to its surroundings, including their difference in orientations and size distribution.

Figure 6(a-f) shows the relations between the annealed and quenched nylon 66 fibers and their birefringence at different temperatures and constant

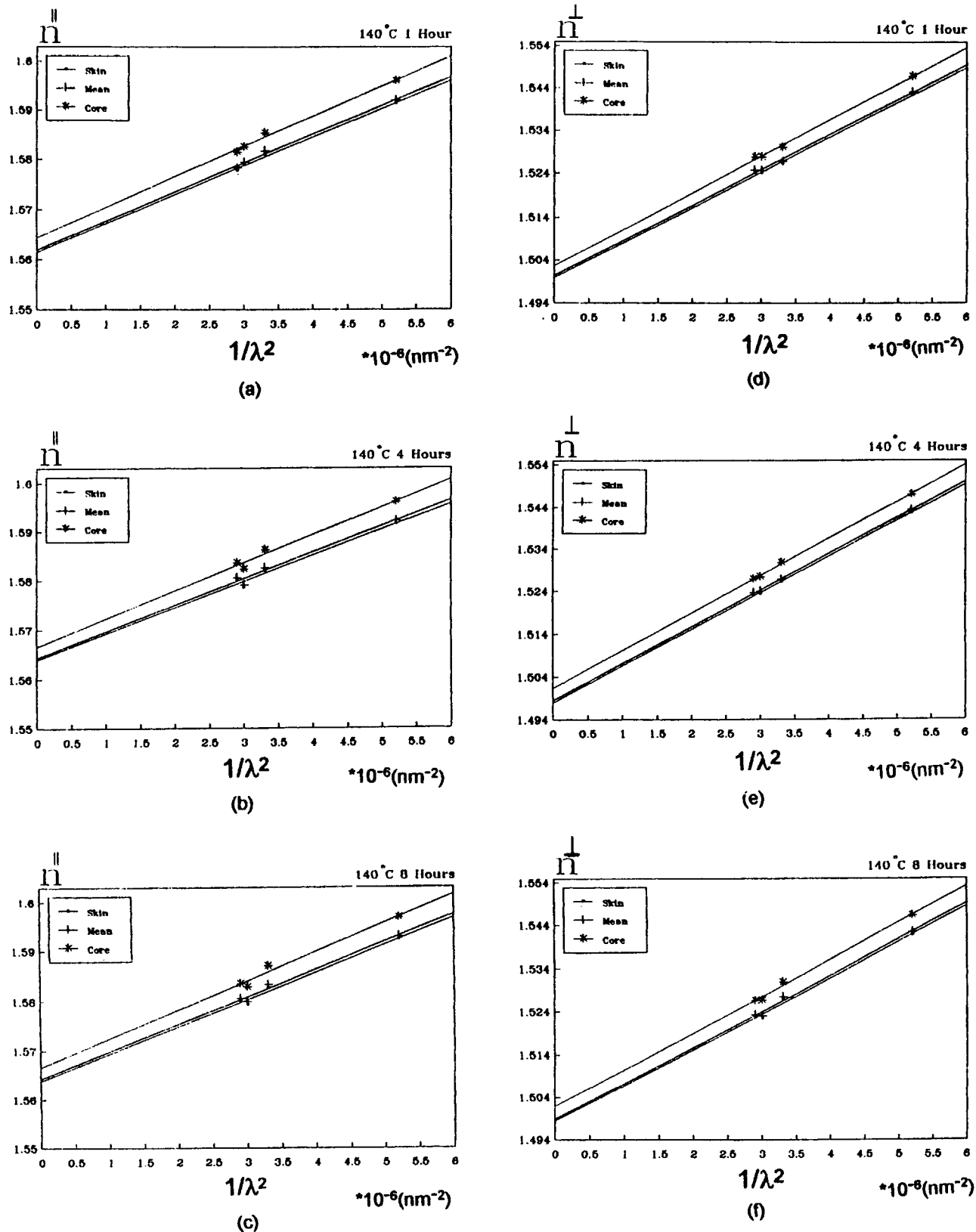


Figure 8 Variation of (a-c)  $n_s^{\parallel}$ ,  $n_c^{\parallel}$ , and  $n_a^{\parallel}$ , and (d-f)  $n_s^{\perp}$ ,  $n_c^{\perp}$ , and  $n_a^{\perp}$  with  $1/\lambda^2$  for annealed nylon 66 fibers at  $140^\circ$  and quenched in coarse ice ( $0^\circ\text{C}$ ) for different annealing times.

**Table III Values of Cauchy's Constants for Untreated and Quenched Nylon 66 Fibers**

State	Layer	Constant "A"		Constant "B" × 10 <sup>3</sup> (nm <sup>2</sup> )	
		A <sup>  </sup>	A <sup>⊥</sup>	B <sup>  </sup>	B <sup>⊥</sup>
Unannealed	Skin	1.5614	1.4988	4.29	7.99
	Mean	1.5623	1.4996	3.64	8.04
	Core	1.5618	1.5016	3.89	8.38
140°C 1 h	Skin	1.5619	1.4998	5.99	7.99
	Mean	1.5624	1.5002	5.97	8.04
	Core	1.5648	1.5026	7.33	8.42
140°C 4 h	Skin	1.5642	1.4986	5.33	8.42
	Mean	1.5646	1.4982	6.27	8.46
	Core	1.5671	1.5016	6.99	8.76
140°C 8 h	Skin	1.5642	1.5998	5.39	8.04
	Mean	1.5648	1.5991	5.37	8.23
	Core	1.5671	1.5024	5.69	8.38

time periods. From these curves, we deduce that a disordered state of orientation was produced by annealing and quenching for different annealing periods.

#### Application of Multiple-beam Fizeau Fringes to Determine Cauchy's Dispersive Formula and the Dispersive Coefficient for Nylon 66 Fibers

Plate 5(a,b) shows multiple-beam Fizeau fringes in transmission for light vibrating parallel and perpendicular to the fiber axis using monochromatic wavelengths of 546.1, 577, and 579, respectively, for untreated nylon 66 fibers. Figures 7(a,b) and 8(a-f) show the relations among  $n_s^{||,⊥}$ ,  $n_c^{||,⊥}$ ,  $n_a^{||,⊥}$ , and  $1/\lambda^2$  for light vibrating parallel and perpendicular to the fiber axis of wavelengths 436, 546.1, 577, and 579 nm. It was constructed to evaluate constants  $A$  and  $B$  of Cauchy's formula<sup>26,27</sup>:

$$n_\lambda = A + B/\lambda^2 \quad (5)$$

The values of Cauchy's constants are given in Table III. According to Cauchy's dispersive formula, we obtain the dispersive coefficient by differentiation:

$$\frac{dn}{d\lambda} = \frac{-2B}{\lambda^3} \quad (6)$$

The resolving power of the fiber layers was also calculated. The results are tabulated in Table IV.

#### Determination of the Principal Polarizability per Unit Volume in the Skin and Core Layers

The polarizability of molecules is the origin of the refractive index of a material. The polarizability is related to the refractive indices by the well-known relation of Lorentz-Lorenz<sup>28,29</sup> which is given by

$$\frac{n^2 - 1}{n^2 + 2} = \frac{4}{3} \pi P \quad (7)$$

where  $P$  is the polarizability per unit volume. Table V gives the calculated results of  $P_s^{||,⊥}$ ,  $\Delta P_s$ ,  $P_c^{||,⊥}$ , and  $\Delta P_c$  for different wavelengths. The obtained results throw light on the variation of the wavelengths with the polarizability, i.e., the polarizability is not a material constant, but depends on the frequency of the wave interactions and layer orientation.

As birefringence yields information about crystallinity and the orientation of the polymer molecular chains, the isotropic refractive index of the medium also gives information about not only the molecular package but also specifications of the medium. Hannes<sup>30</sup> used the following formula:

$$n_{\text{iso}} = \frac{1}{3} (n^{||} + 2n^\perp) \quad (8)$$

to estimate a relationship showing the crystallization inhomogeneity for some types of polymers. The obtained values of  $n_s^{||,⊥}$ ,  $n_c^{||,⊥}$ , and  $n_a^{||,⊥}$  for the interfer-

**Table IV Average Value of Dispersive Power of Untreated and Quenched Nylon 66 Fibers**

State	Layer	$dn^{  }/d\lambda$	$dn^\perp/d\lambda$
Unannealed	Skin	$-5.27 \times 10^{-5}$	$-9.81 \times 10^{-5}$
	Mean	$-4.47 \times 10^{-5}$	$-9.87 \times 10^{-5}$
	Core	$-4.78 \times 10^{-5}$	$-1.03 \times 10^{-4}$
140°C 1 h	Skin	$-7.56 \times 10^{-5}$	$-9.81 \times 10^{-5}$
	Mean	$-7.33 \times 10^{-5}$	$-9.87 \times 10^{-5}$
	Core	$-9.00 \times 10^{-5}$	$-1.03 \times 10^{-4}$
140°C 4 h	Skin	$-6.55 \times 10^{-5}$	$-1.03 \times 10^{-4}$
	Mean	$-7.69 \times 10^{-5}$	$-1.04 \times 10^{-4}$
	Core	$-8.58 \times 10^{-5}$	$-1.07 \times 10^{-4}$
140°C 8 h	Skin	$-6.62 \times 10^{-5}$	$-1.03 \times 10^{-4}$
	Mean	$-6.59 \times 10^{-5}$	$-1.01 \times 10^{-4}$
	Core	$-6.98 \times 10^{-5}$	$-1.03 \times 10^{-4}$

**Table V** Values of Polarizability per Unit Volume of Untreated and Quenched Nylon 66 Fibers Different Wavelengths (577, 579, 546.1, and 436 nm)

State	Layer	$P^{\parallel}$ Wavelength (nm)				$P^{\perp}$ Wavelength (nm)				$\Delta P$ Wavelength (nm)			
		577	579	546.1	436	577	579	546.1	436	577	579	546.1	436
Untreated	Skin	.0791	.0798	.07868	.0787	.0730	.0749	.07289	.07285	.0061	.0049	.0038	.0059
	Core	.0799	.0804	.0791	.0792	.0735	.0755	.0734	.0733	.0064	.0049	.0058	.0059
140°C 1 h	Skin	.0795	.0807	.0792	.0793	.0733	.0752	.073	.0731	.0063	.0055	.0061	.0062
	Core	.0800	.0812	.0796	.0797	.0733	.0757	.0735	.07347	.0068	.0055	.0061	.0062
140°C 4 h	Skin	.0796	.0807	.0794	.0793	.0733	.0752	.0738	.0729	.0063	.0055	.0064	.0064
	Core	.0801	.0812	.0798	.0797	.0738	.0757	.0734	.0733	.0063	.0055	.0069	.0063
140°C 8 h	Skin	.0797	.0808	.0794	.0793	.0734	.0751	.0728	.0729	.0063	.0057	.0066	.0065
	Core	.0802	.0813	.0798	.0797	.0797	.0738	.0756	.0734	.0064	.0057	.0074	.0064



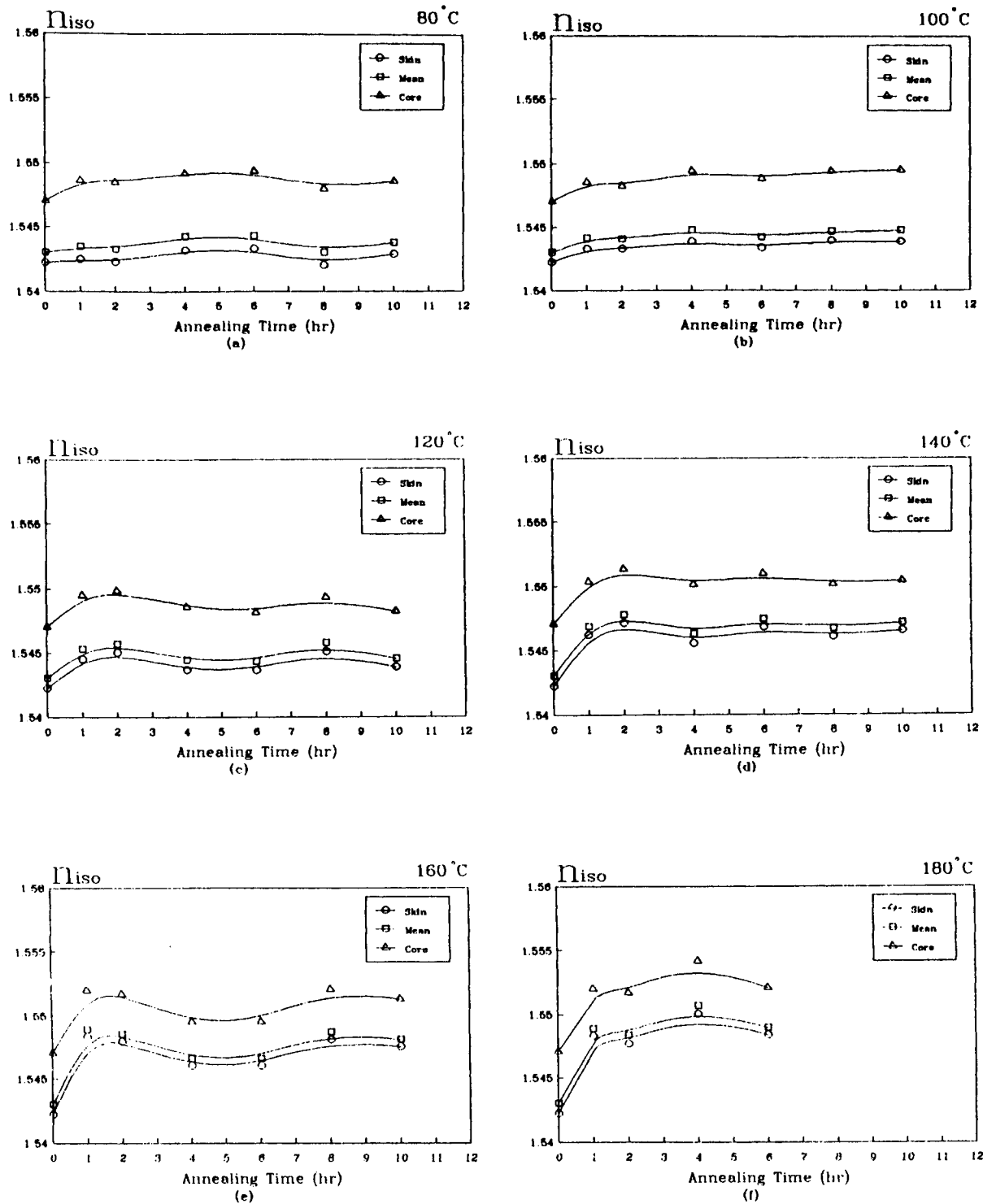
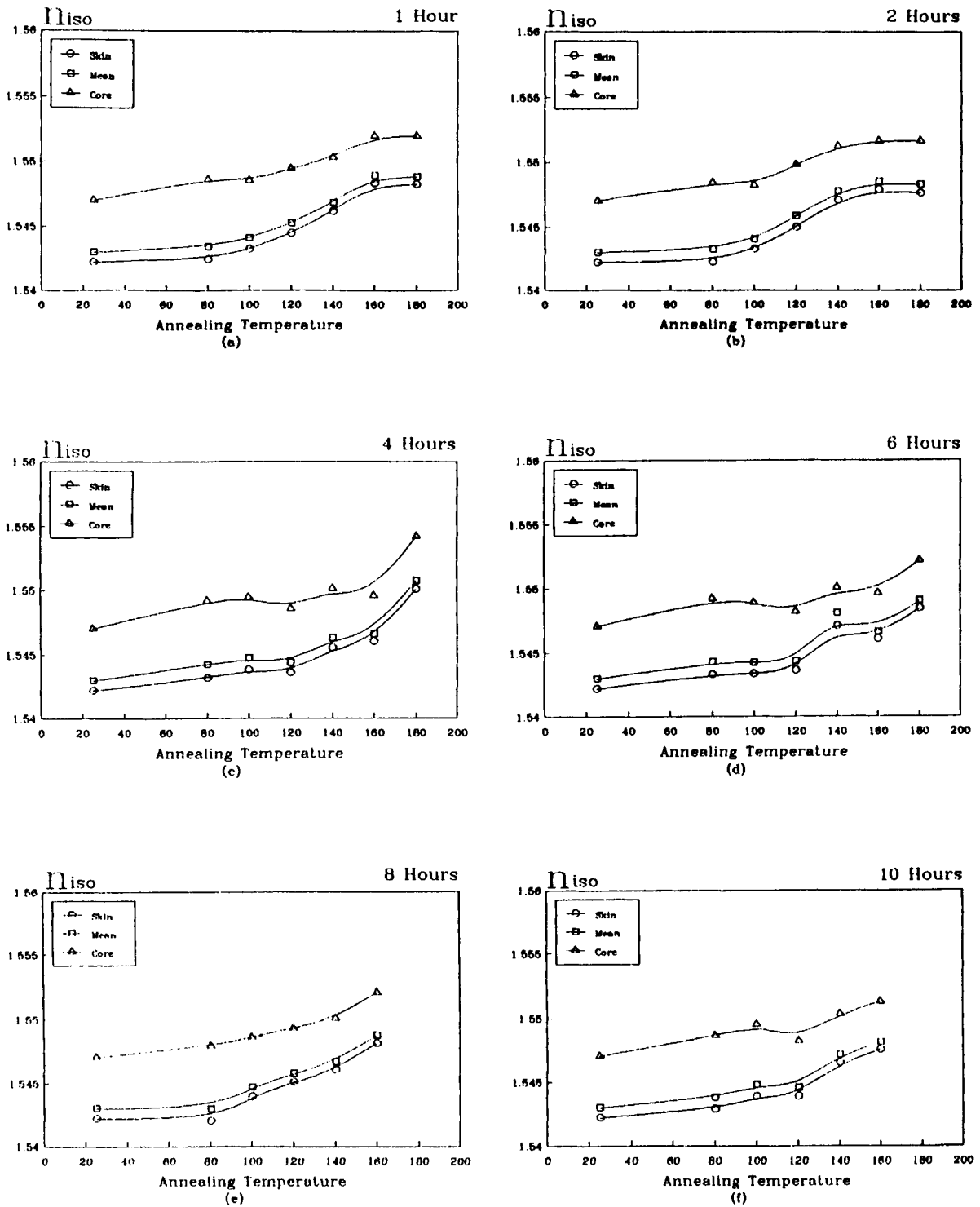


Figure 9 (a-f) Relation between quenched nylon 66 fibers for different annealing periods (1-10 h) and for constant annealing temperatures with isotropic refractive indices.



**Figure 10** (a-f) Relation between quenched nylon 66 fibers for different annealing temperatures (80–180°C) and different annealing periods with isotropic refractive indices.

ometric techniques are used with eq. (8) to determine the isotropic refractive index values for quenching nylon 66 fibers.

Figure 9(a-f) shows the behavior of  $n_{(iso)s}$ ,  $n_{(iso)c}$ , and  $n_{(iso)a}$  of quenched nylon 66 fibers with different annealing times and constant annealing temperatures.

Figure 10(a-f) shows the behaviors of  $n_{(iso)s}$ ,  $n_{(iso)c}$ , and  $n_{(iso)a}$  of quenched nylon 66 fibers with different annealing temperatures (80–180°C) for constant annealing periods. The curves reflect the new reorientations due to the thermal treatments.

## CONCLUSIONS

From the previous discussion and representations, the following conclusions may be drawn:

1. The macromolecular structure of nylon 66 is strongly affected by the isothermal annealing and quenched treatment conditions.
2. The obtained results throw light on the importance of the effect of annealing temperature, time, and quenching in coarse ice pieces on the optical properties of nylon 66 fibers. The results may be used for monitoring the isothermal process of the polymer fiber.
3. Change in the isotropic refractive indices is related to the degree of order and crystallinity of the fiber as well as to the density of sample  $[(n_{iso} - 1)/\rho] = K$ .
4. The study of the change of  $n_s^{\parallel\perp}$ ,  $n_c^{\parallel\perp}$ ,  $n_a^{\parallel\perp}$ ,  $\Delta n_s$ ,  $\Delta n_c$ , and  $\Delta n_a$  with respect to the annealing and quenching process clarifies that the isothermal properties of the structure in a direction perpendicular to the fiber axis differ from those in an axial direction, which is expected for an anisotropy medium.
5. The value of the swelling factor for different liquids depends on the isothermal treatments (annealing and quenching) and also on the nature of the absorbent liquids and the chemical structure of the fiber.
6. Measuring the absorption factor throws light on the degree of the crystalline and amorphous areas, and, in fact, all degrees of order and disorder areas exist.
7. From the several results obtained for the thermal effect of skin and core at the same conditions, it was found that the flow of molecules in the skin differs from that of the core. So, considerable molecular flow can take

place in the skin and core if the temperature or time is sufficiently increased.

8. Thermal treatment and quenching varied the degree of orientation (crystallinity) and produced a disorder state for different conditions.
9. Quenching affects slightly the transport properties of the fibrous structure due to the quenching.
10. Changes due to quenching in the orientation accompanied by a change of crystallinity indicate also a change of other physical and mechanical properties, which needs further studies.
11. The thermal treatment and quenching process affects the color of fiber material due to the oxidative properties of oxygen.
12. As crystallinity and orientation increase and go to the disordered state, the dyeability of quenched nylon 66 fibers is expected to go to variable states and to decrease.

Since  $\Delta n_s$ ,  $\Delta n_c$ ,  $\Delta n_a$ , and other optical parameters are a consequence of the material being thermally treated, optical anisotropy is a consequence of thermal anisotropy. We conclude that multiple-beam Fizeau fringes offer a valuable technique for gaining information on the thermal and quenched material and on the optical properties of the fibers.

## REFERENCES

1. P. S. Theocaries, G. B. Philis, and C. H. Blontzen, *J. Phys. E Sci. Instrum.*, **8**, 611 (1975).
2. R. C. Faust, *Proc. Phys. Soc. B*, **65**, 138 (1952).
3. N. Barakat, *Text. Res. J.*, **41**, 167 (1971).
4. S. C. Simmens, *Nature*, **181**, 1260 (1958).
5. A. A. Hamza, I. M. Fouda, K. A. El-Farahaty, and Y. K. M. Badawy, *Text. Res. J.*, **50**, 215 (1980).
6. A. A. Hamza, T. Z. N. Sokkar, and M. A. Kabeel, *J. Phys. D Appl. Phys.*, **18**, 1773 (1985).
7. M. Pluta, *Opt. Acta*, **18**, 661 (1971).
8. I. M. Fouda, M. M. El-Tonsy, and K. A. El-Farahaty, *Arab Gulf J. Sci. Res.*, **8**(2), 60 (1990).
9. W. Zúrek and S. Zakrzewski, *J. Appl. Polym. Sci.*, **28**, 1277 (1983).
10. N. Barakat and A. A. Hamza, *Interferometry of Fibrous Material*, Adam Higler, Bristol, 1990.
11. A. A. Hamza, I. M. Fouda, T. Z. N. Sokkar, M. M. Shahin, and E. A. Seisa., *Polym. Test.*, **11**, 297 (1992).
12. I. M. Fouda and M. M. El-Tonsy, *J. Mater. Sci.*, **25**, 121 (1990).
13. I. M. Fouda and M. M. El-Tonsy, *J. Mater. Sci.*, **25**, 4752 (1990).

14. I. M. Fou da, M. M. El-Tonsy, and A. M. Shaban, *J. Mater. Sci.*, **26**, 5085 (1991).
15. A. A. Hamza, I. M. Fou da, M. M. El-Tonsy, and F. M. El-Sharkawy, *J. Appl. Polym. Sci.*, to appear.
16. W. O. S. Statton, *J. Polym. Sci. A*, **210**, 1587 (1992).
17. F. Decandia and V. Vittoria, *J. Polym. Sci. Phys. Ed.*, **23**, 1217 (1985).
18. G. William, P. Perkins, and S. R. Porter, *J. Mater. Sci.*, 2355 (1977).
19. A. Z. Zachariades and S. Porter, *The Strength and Stiffness of Polymers*, Marcel Dekker, New York, Basel, 1983, p. 121.
20. W. Howard, J. R. Starkweather, E. M. George, J. E. Hansen, T. M. Roder, and R. E. Brooks, *J. Polym. Sci.*, **21**, 201 (1956).
21. H. Wycoff, *J. Polym. Sci.*, **62**, 83 (1962).
22. M. M. El-Nicklaway and I. M. Fou da, *J. Text. Inst.*, **71**, 252-256 (1980).
23. S. M. Curry and A. L. Schawlow. *Am. J. Phys.*, **42**, 12 (1972).
24. J. V. Brancik and A. J. Datyner, *Text. Res. J.*, **47**, 662 (1972).
25. J. H. Mckan, *Text. Res. J.*, **35**, 242 (1965).
26. W. E. Ernest, *Optical Crystallography*, Wiley, New York, 1979, p. 112.
27. N. Subrahmanyam, *Brijlal, A Text Book of Optics*, S & C, 1979, p. 93.
28. J. R. Samuels, *Structured Polymer Properties*, Wiley, New York, 1974, pp. 50-60.
29. W. I. Ward, *Structure and Properties of Oriented Polymers*, Applied Science, London, 1975, p. 57.
30. H. Hannes, *Z. Z. Kolloid Polym.*, **250**, 765 (1972).

Received April 5, 1995

Accepted October 6, 1995